IET Research Journals

Accepted Version, by IET Smart Grid journal on 21st Feb 2019.

IET Journals
The Institution of Engineering and Technology

ISSN 1751-8644
doi: 0000000000
www.ietdl.org

Dynamic Charging of Electric Vehicles Integrating Renewable Energy: A Multi-Objective Optimisation Problem

Harry Humfrey[†], *Hongjian Sun*[‡], *Jing Jiang*[*]

[†] *Business School, Imperial College London, SW7 2AZ, United Kingdom*
[‡] *Department of Engineering, Durham University, Durham, DH1 3LE, United Kingdom*
[*] *Department of Mathematics, Physics and Electrical Engineering, Northumbria University, Newcastle upon Tyne, NE1 8ST, United Kingdom*
** E-mail: jing.jiang@Northumbria.ac.uk (corresponding author)*

Abstract: Dynamically charging electric vehicles (EVs) has the potential to significantly reduce range anxiety and decrease the size of battery required for acceptable range. However, with the main driver for progressing EV technology being the reduction of carbon emissions, consideration of how a dynamic charging system would impact these emissions is required. This paper presents a demand side management method for allocating resources to charge EVs dynamically considering the integration of local renewable generation. A multi-objective optimisation problem is formulated to consider individual users, an energy retailer, and a regulator as players with conflicting interests. A 19% reduction in the energy drawn from the power grid is observed over the course of a 24-hour period when compared with a first-come-first-served allocation method. This results in a greater reduction in CO_2 emissions of 22% by considering the power grid's make-up at each time interval. Furthermore, a 42% reduction in CO_2 emissions is achieved compared to a system without local renewable energy integration. By varying the weights assigned the players' goals, the method can reduce overall demand at peak times and produce a smoother demand profile. Finally, the described benefits do not come at the expense of user experience. In fact, system fairness is shown to improve with an average Gini coefficient reduction of 4.32%.

1 Introduction

Electric vehicles (EVs) are becoming increasingly prevalent in transportation. In the UK, the adoption rate has been staggering, with there being 20 times more registered EVs in 2017 than in 2012 [1]. The move away from conventional fossil-fuelled vehicles is accelerating as advances in related technologies are making EVs financially viable [2]. It is expected that this trend will continue and this will certainly impose extreme strains on existing power infrastructure. In the National Grid's Future Energy Scenarios report [3], it was recognised that UK peak energy demand could grow by 50% purely from increased EV penetration by 2045 - compounded by the homogeneity of the population's charging habits. Moreover, with advancements in driverless car technology, it is expected that the number of cars on the road will increase as the mode of transport becomes more attractive and, through ride-sharing options, each car spends more time on the road [4, 5]. There exist, however, a number of obstacles that may hinder the success of EVs. Due to limited battery capacities and the sporadic availability of charging stations along transport routes, drivers are experiencing significant range anxiety issues [6]. For EV producers, this remains an extremely challenging element of design as large battery packs, as are required for acceptable range, continue to dominate both the cost and mass of vehicles [7]. Note that for the entirety of this paper, the term EV will be used to encapsulate both battery-only and hybrid electric vehicles.

A promising solution to the problems facing EVs is to implement dynamic on-road charging. Wireless Power Transfer (WPT) can be achieved using primary coils beneath the road surface and secondary coils inside the vehicles themselves. Through applying power to the primary coils when the EVs are positioned above, WPT can be achieved with an overall transfer efficiency in the range of 60-75% [8]. Such a system could significantly reduce range anxiety issues as users would be able to charge EVs whilst travelling and, in addition, could help to reduce the effects of concurrent EV charging routines.

The WPT technology also has the potential to significantly reduce battery size, as the capacity required to travel along routes with dynamic charging availability would materially decrease and, as such, so would the price of the EVs [9]. Moreover, in the US whilst 85.3% of roads are classified as "small local", 85.0% of all miles driven are on primary or secondary roads with a split of 69.7% and 15.4%, respectively [10]. This suggests that it is possible to impact a large number of users by targeting specific frequently used roads.

There are currently a number of commercial systems using WPT technology such as the Online Electric Vehicle (OLEV) system in use in several cities across South Korea [11]. Though such projects have been proven to be largely successful for small scale public transport systems, this concept comes with a number of challenges to overcome when considering a larger, more volatile system of individual EVs. Since the amount of energy that the power grid can supply at any one time is not unbounded and nor indeed is the energy that can be drawn from a given transformer, careful consideration of how to distribute the available energy to the participating EVs is required. This paper outlines a demand side management (DSM) technique for the allocation of resources that takes into account individual EV requirements and offsets peak demand by modelling the make-up of the electricity supply throughout the day and its effect on system utility.

The remainder of this paper is organised as follows. Section 2 presents an overview of literature relevant to WPT and DSM as they apply to EVs. In Section 3 a general overview of the system is described and assumptions are stated. Formulation of a multi-objective optimisation problem is given in Section 4 and numerical results are discussed in Section 5. Finally, conclusions are drawn and opportunities for future work are identified in Section 6.

2 Literature Review

This section presents an overview of relevant literature. Section 2.1 interrogates system hardware and communication infrastructure requirements, Section 2.2 discusses DSM as it is applied to EV charging and Section 2.3 highlights gaps in the research and the contributions made by this paper.

2.1 Wireless Charging of EVs

The functionality of a dynamic road system (DRS) will ultimately be shaped by hardware limitations. WPT typically exhibits highly fluctuating transfer efficiencies based on coil alignment. This could pose a serious problem when there is relative movement between primary and secondary coils as in the case of the DRS. However, progress has been made in this area and, with the arrangement discussed in [12], high transfer efficiencies have been demonstrated over a range of different alignment positions. Furthermore, with the advent of autonomous driving technology, lane alignment will cease to be an issue with localisation accuracies of under 3cm expected [13]. The ultra-low communication latency requirements of a DRS were outlined in [14] and the need for vehicle authentication and accurate positioning was described. More recently, dedicated short range communication systems have been shown to offer a latency in such a system of under 6ms with the use of detection sensors before each charging pad [15]. This method was explored further in [16], where a novel method of exchanging cryptocurrency with each charging pad to circumvent authentication issues and reduce the frequency of information exchange between EVs and the road was described.

2.2 Demand Side Management

DSM can be used to ensure equilibrium between demand and supply in power systems. The application of DSM in static EV charging is a mature area of study. However, when applying DSM to dynamic charging, the approach must be updated to factor in the operational requirements of the DRS [17]. When charging dynamically, charging sessions last only a few milliseconds [18] and, therefore, the charging service must be applied without delay. By contrast, in the static case, users can tolerate significant delay when starting to charge. As a result, the computational complexity of the DSM optimisation must be materially reduced to be effective. In addition, the length of time that a given EV can charge is unknown, as opposed to a generally known period in the static case [19]. As a consequence, DSM methods which aim to optimise over long time periods would be ineffective. Furthermore, due to the much shorter overall charging period, the charging rates applied to the EVs must be higher. This results in a significant strain on the power grid. Therefore, development of a dynamic WPT specific DSM method is necessary to address the unique characteristics present in the dynamic charging environment.

Scheduling the charging of EVs fleet to provide ancillary services has been an active area of research [20–28]. However, these almost entirely focus on the static charging case, where multiple EVs can be scheduled over a long charging period. Work done in extending this to the dynamic case, where charging periods are much shorter, is limited.

DSM methods can largely be split into two categories: centralised and decentralised. In the former, an aggregator typically acts as an energy manager between utility companies and consumers. As such, the aggregator collects constraints from participants, performs optimisation tasks and broadcasts the resulting decisions the players [29]. In the decentralised case, however, each participant optimises locally.

A centralised algorithm was presented in [21] with the aim of reducing peak demand. Here the author noted that the time slot allocation method proposed may be extended to the dynamic case simply by optimising for smaller time slots. However, this system organises EVs into charging slots based on their calculated priority. In a system where EVs can spend only a short period of time on the road and total power transfer is significantly limited, this method would leave many users dissatisfied.

Game theoretic approaches, both centralised and decentralised, were discussed in [22–27], where each EV is modelled as a player in a game with the objective of maximising their utility subject to a number of constraints and the current price of electricity. Non-cooperative games are presented in [22–25], and compared with optimal control theories in [30]. In non-cooperative games, the players' utility functions are modelled differently. In [23], EV utility was modelled as a non-decreasing concave function to include the battery state-of-charge, electricity price and charging decisions of other participating EVs. In the decentralised algorithm outlined, the sharing of charging information between road users is required. This could pose serious security concerns and, as such, this approach should be avoided where possible. A Stackelberg game was considered in [26, 27], where the electricity provider acts as the game leader. Here the power grid sets the price to maximise profits, given that it knows how each player will react to a change in price, which is then broadcast to the other players.

A method for defining an objective function of the carbon burdens associated with electricity generation as a function of the various fuel types being used was outlined in [31] and in [32], the potential to supplement the DRS with local renewable generation was identified. To maximise the benefits of all participants in above EVs charging, a multiobjective problem (MOP) should be formulated. To solve MOP, various heuristic approaches were studied in the literature [33–37]. For example, applying NGSA-II algorithm [33] and artificial immune algorithm [37] could lead to a Pareto optimal set for a MOP.

2.3 Research Gaps and Contributions

Much of the research carried out to date relating to EV resource allocation has been focused on static demand scheduling with the objective of smoothing the demand curve or minimising cost. It is recognised, therefore, that there is a need to develop a DSM model for dynamic charging scenarios for the future low-carbon transport system. This paper builds on the objective functions outlined in [26] in formulating a centralised multi-objective optimisation problem for the DRS. Emphasis throughout is on the modelling of a workable system and not on the application of the optimisation techniques themselves. The key contributions made by this paper are as follows:

- A DSM method is proposed for managing the operation of a DRS. In doing so, individual charging rates are allocated based on each user's need to charge. Given the short charging time, limitations on transfer rate and the uncertainty of how long each EV will remain on the road, this approach distributes resources between users more fairly when compared to a charge scheduling approach.
- A regulator is introduced to the system model. This player acts so as to reduce the amount of power drawn from the grid when generation is strained and, as such, means the DRS can act as a variable load. This feature is a significant benefit when considering the strain on future power grid infrastructure as a result of widespread EV charging and indeed, on the resultant CO_2 emissions.
- Local renewable energy generation is built into the system model and the associated reductions in CO_2 emissions are presented. Furthermore, it is demonstrated that significant reductions in carbon emissions can be observed with a relatively small installed local generation capacity.

3 System Model

The implementation of DRSs across the UK was investigated in a Highways England feasibility study [8]. Here, it is recognised that the most appropriate method would be to have a dedicated charging lane along a motorway. In this case, charging pads 40m in length are embedded in the road surface with 5m spacings between sections, and each section is connected to a road side unit (RSU) which controls the road. An overview of the system is given Figure 1.

It can be seen that, in front of each pad, there is a sensor to recognise the approaching car. This may be used to track the positions of vehicles on the road and facilitate vehicle authentication or cryptocurrency exchanges as mentioned in Section 2.2. Given that each pad may only charge a single vehicle at a time, a minimum spacing between each EV of 40m is required. A constant speed of 70mph, the UK motorway speed limit, is defined such that the spacings between cars remain constant. Since there is a maximum of one car to a pad, this allows the RSU to apply different charging rates to each car on the road.

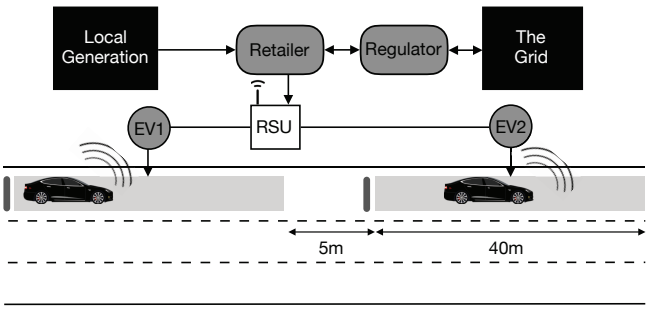

Fig. 1: Overview of the DRS showing the EV users, energy retailer, regulator and RSU aggregator. Directions of arrows indicate the possible flows of energy

The DRS may be supplied by the grid and also by local renewable generation such as solar or wind. In an instance where local generation exceeds the consumption of the road, this may also be sold back to the grid. The system is represented such that the RSU aggregates information from three players. The electricity retailer wants to maximise profits made from selling electricity to EVs. A regulator is defined that can act so as to reduce the electricity received from the grid when the generation system is strained. Finally, each EV's willingness to charge is dependent on the price of electricity and other factors such as state-of-charge.

In the system considered, the RSU performs the optimisation and operates the road. As such, the method can be considered a centralised scheme. Here, the RSU aggregates the requirements of the system stakeholders. Accordingly, this requires EVs to send relevant parameters to the RSU when approaching the road and whenever these parameters change. A centralised system best applies to the DRS as it eliminates the need for correspondence between individual EVs. In the DRS, and particularly because the frequency of users passing through the system is high, such communication could cause significant security concerns. Furthermore, as far as the system can be characterised as a single strictly convex function to be optimised, the necessary computing power for centralised optimisation should not be excessive.

Given the unique nature of dynamic charging, the optimisation of charging schedules typically used in the static case is not applicable for resource allocation. This paper, therefore, outlines a real time DSM method whereby users are allocated charging rates in accordance with their willingness to charge. With a continues scale of possible charging rates that are readily variable, this approach is better suited to the DRS.

For the system described, optimisation is required at a high rate. Namely, charging rates must be computed every time the system changes due to a new car entering the road, a car leaving the road, updated local generation information, or changes to the grid make-up. It is recognised that this optimisation rate, coupled with the high switching frequency required to provide high speed EVs with unique charging rates, would come at a significant cost to the implementation of the system. However, this paper is concerned with developing an effective method of meeting the needs of all parties for a future DRS and, as such, the cost of implementation is not considered.

4 Methodology

All of the parties involved have their own objectives and corresponding constraints. Since the players' objectives are conflicting, they are modelled here separately and combined in a multi-objective optimisation problem in section 4.4. The model described uses a real time optimisation approach and, as such, optimises for the current system state, as opposed to optimising over a given time period. Accordingly, real time pricing is used in every time step.

4.1 Retailer Modelling

The retailer in the dynamic road system sells electricity to participating EVs. The objective, therefore, is formulated to maximise its profits. The utility function of the retailer is given by,

$$L(\boldsymbol{X}, \boldsymbol{P}, p) = p \sum_{n=1}^{N} (x_n + P_n), \tag{1}$$

where $\boldsymbol{X} := [x_1, x_2, ..., x_N]$, and $\boldsymbol{P} := [P_1, P_2, ..., P_N]$, are vectors of the electricity demanded by each EV from the grid and from renewables, respectively, in a given time step, p is the price per unit energy, N is the number of EVs currently on the road and n is the EV index. The demand from renewables,

$$P_n = \min \left\{ \frac{P_t}{N},\ T_n^{(max)},\ \frac{C}{N} \right\} \tag{2}$$

where P_t is the total power available from renewables, $T_n^{(max)}$ is the maximum transfer rate of the EV and C is the transformer capacity. In this manner, as far as system constraints allow, each vehicle is allocated an equal share of the available renewable supply automatically with the DSM techniques only applying to the energy supplied from the grid, $\boldsymbol{X}$. Since the retailer sells electricity from both sources, this is reflected in the utility function,

$$L(\boldsymbol{Y}, p) = p \sum_{n=1}^{N} y_n, \tag{3}$$

where, $y_n = x_n + P_n$, is the total energy transfer rate of EV n and $\boldsymbol{Y} := [y_1, y_2, ..., y_N]$.

4.2 Regulator Modelling

The equivalent production of CO_2 for every unit of energy produced by the grid was quantified in [31], where the Electricity Grid Carbon Factor (EGCF) is defined as,

$$EGCF = \frac{\sum_{m=1}^{M} C_m E_m}{\sum_{m=1}^{M} E_m}, \tag{4}$$

where M is the total number of fuel types, C_m is the CO_2 intensity of fuel m and E_m is the generated energy corresponding to m. Approximate values of CO_2 intensity for fuel sources that make up the vast majority of power grid generation are given in Table 1. To formulate the regulator's utility, a normalised carbon factor, f, is defined as a measure of how carbon-heavy the grid electricity is at a given instant,

$$f = \frac{EGCF}{EGCF_{nom}}, \tag{5}$$

where $EGCF_{nom}$ is some nominal value. Since the objective of greater EV penetration, and hence the implementation of DRSs, could broadly be considered to be lowering the carbon footprint of the transportation sector, the regulator modelling should account for this. The goal of the regulator, which could be a government body such as the Department for Energy and Climate Change (DECC), is to limit the use of high carbon factor electricity. Accordingly, the regulator's utility function is given by,

$$R(\boldsymbol{X}, f) = \begin{cases} \sum_{n=1}^{N} x_n^2 (1 - f), & \text{if } f > 1 \\ 0, & \text{otherwise.} \end{cases} \tag{6}$$

It can be seen that, for $f > 1$, the utility of the regulator is negative and decreases quadratically with system demand. Defining the regulator utility as non-positive makes sense in the scenario considered since a body such as the DECC would not benefit from any level of power usage but could be negatively affected by increased demand and high carbon factor, f.

The regulator will, therefore, lower the overall electricity transferred when, for instance, coal makes up a significant proportion

of the generation. It follows from (5) and (6) that the choice of $ECGF_{nom}$ will define the level of CO_2 production at which the regulator begins to influence demand. For this paper, $ECGF_{nom}$ is taken as the average of the daily EGCF values but it is recognised that this could be changed to represent a different critical value.

4.3 Customer Modelling

The utility of each EV, based on that proposed in [26], is a non-decreasing quadratic function,

$$u_n(y_n,p)=\begin{cases} y_n(b_n-p)-\frac{1}{2}s_n y_n^2, & \text{if } T_n^{(min)}\le y_n<y_n^* \\ y_n^*(b_n-p)-\frac{1}{2}s_n y_n^{*2} & \text{if } y_n^*\le y_n<T_n^{(max)} \\ 0, & \text{otherwise,}\end{cases} \tag{7}$$

where y_n^* is the maximum value of the quadratic function, b_n is the available battery capacity, s_n is the satisfaction parameter and $T_n^{(min)}$ and $T_n^{(max)}$ are the minimum and maximum charging rates of the n^{th} EV, respectively. Modifications have been made to the definitions of the terms as proposed in [26]. The parameter, b_n, was originally defined as the total battery size but this change has been made to put greater emphasis on each user's potential to charge rather than their total battery size. The satisfaction parameter, s_n, is a measure of how much an EV will benefit from consuming an additional unit of energy. Where this had previously not explicitly been defined, here it is formulated as,

$$s_n=\frac{\nu_n+\mu_n}{2}, \tag{8}$$

where $\mu_n\in[1,2]$ is a user-defined parameter that can be varied by the driver to further describe their willingness to charge which could conceivably be varied while driving. Clearly, selecting a low value increases one's willingness to charge which may result in accepting electricity at a high tariff. Additionally,

$$\nu_n=1+\min\left\{\frac{d_n}{d_n^{(max)}},\,1\right\}, \tag{9}$$

where d_n is the distance a user is away from their destination and $d_n^{(max)}$ is the maximum distance that user can travel on its current charge level. This parameter is designed to reflect how different users' utilities depend on their travel plans. It follows that, for a user that has a short distance to travel, they will have less need to charge than those with far to travel. Constraining $\nu_n\in[1,2]$ prevents users with a large distance to travel from dominating the system demand.

The assumption of non-decreasing EV utility is reasonable here since no user's utility would be expected to decrease for higher transfer rates. Figure 2 shows this in graphical form for a random set of four EVs. It can be seen that there are minimum and maximum transfer rates between which EVs can benefit, as defined by hardware constraints, and a flat profile may be observed at high transfer rates. Since the power available from local renewable generation is distributed equally amongst participating EVs, the optimisation problem is on the sections of curve after P_n for the nth EV. Nonetheless, each user does not distinguish between types of generation and, as such, utilities reflect this.

Table 1 CO_2 intensities of fuel sources that make up the majority of UK power grid generation [31] [38]

Fuel Type	CO_2 Intensity, C_m (gCO_2eq/kWh)
Coal	800
Oil	650
Open Cycle Gas	526
Combined Cycle Gas	427
Biomass	100
Wind	57
Solar PV	50
Nuclear	23
Hydro	7

The objectives of the participating EVs can be aggregated to form a single function to be optimised:

$$U(\boldsymbol{Y},p)=\sum_{n=1}^{N}u_n(y_n,p). \tag{10}$$

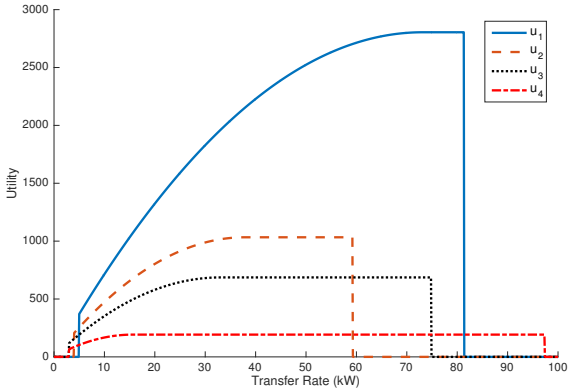

Fig. 2: Non-decreasing utility functions given by (7) for four EVs

4.4 The Multi-Objective Optimisation Problem

The overall function to be maximised is given by,

$$F(\boldsymbol{X},\boldsymbol{P},p,f)=\alpha\frac{L(\boldsymbol{Y},p)}{L_{max}}+\beta\frac{R(\boldsymbol{X},f)}{R_{max}}+\gamma\frac{U(\boldsymbol{Y},p)}{U_{max}}, \tag{11}$$

where L_{max}, R_{max} and U_{max} are the maximum possible values of the respective utility functions and are used to normalise the outputs. The variables α, β and γ represent weights to be given to each player in the optimisation problem such that $\alpha+\beta+\gamma=1$.

Each of the players' interests are conflicting. Clearly, EV users' and the retailer's utilities will both increase with higher charging rates. However, the converse is true for the regulator, whose utility decreases quadratically with charging rate. Moreover, since the overall power drawn by the DRS is bounded by the transformer capacity, individual EVs can also be said to have conflicting interests; for a given EV to receive a higher rate when the transformer capacity is reached, other EVs in the system must reduce their demand to accommodate.

It follows that the greater the weight given to a player's utility, the greater effect their goals have on the optimised solution. In this system, the regulator, who may be the DECC, sets these weights. It is assumed, therefore, that this regulator will not act selfishly but rather to increase system performance in a pre-determined manner.

There are a number of potential approaches for optimising the weights in order to equilibrate the conflicting interests such as NGSA-II [33] or various heuristic approaches utilised in [34–36]. However, this is not the focus of this study. Instead, the primary objective is the development and simulation of a workable DSM method for the future DRS and, as such, this it is left for future work. For the entirety of this report, specific configurations are used to demonstrate the action of the system, but these do not necessarily represent optimal solutions. Importantly, player weights would not need to be optimised frequently and it is envisioned that these could be set in intervals. For example, peak, off-peak and super off-peak configurations. In doing so, the computational complexity and, hence, the fast operation of the system would not be compromised.

Since L, R and U are convex functions within the prescribed limits, the weighted sum of these functions, F, is also convex. The optimisation problem can be expressed as,

$$\begin{aligned} \max_{\boldsymbol{X},\, p} \quad & F(\boldsymbol{X}, \boldsymbol{P}, p, f) \\ \text{subject to} \quad & \sum_{n=1}^{N} y_n \leq C \\ & T_n^{(min)} \leq y_n \leq T_n^{(max)} \text{ or } y_n = 0, \forall\ n \in \boldsymbol{N} \\ & p_{min} \leq p \leq p_{max} \end{aligned} \tag{12}$$

where $\boldsymbol{N} := [1, 2, ..., N]$, C is the transformer capacity and p_{min} and p_{max} are the limits on the price that can be charged for a unit of electricity as defined by the electricity provider's costs and government policy, respectively.

In order to realise the system described, interaction between the RSU and the players is required. Specifically, each EV must send the following parameters when entering the road: b_n, s_n, $T_n^{(min)}$ and $T_n^{(max)}$. In addition, for long stretches of road in which EVs can expect to obtain a significant amount of charge, b_n and s_n would also need be updated. The retailer must update p_{min} and p_{max} when these change but here these limits are assumed constant. Finally, the regulator is required to update the carbon factor, f, as the grid conditions vary. Notably, the RSU is not required to send any information back to the players but must track the positions of the EVs and apply appropriate charging rates.

4.5 Schematic Overview

The multi-objective optimisation problem outlined in Section 4.4 must be solved when a system parameter changes. The outputs of the optimisation problem are the individual charging rates assigned to each EV within the system, and the price of electricity. As such, the formulation of the optimisation problem, outlined in Sections 4.1 - 4.4 defines the action of the DSM method; the system demand is modified in accordance with user need-to-charge, the carbon factor of the generation system, and the bounds on the minimum and maximum possible electricity price. A schematic overview of the process is given in Figure 3. Diamonds are used to represent questions about the state of the system, blue and red arrows indicate positive and negative responses, respectively, and rectangular boxes indicate an action the system must take.

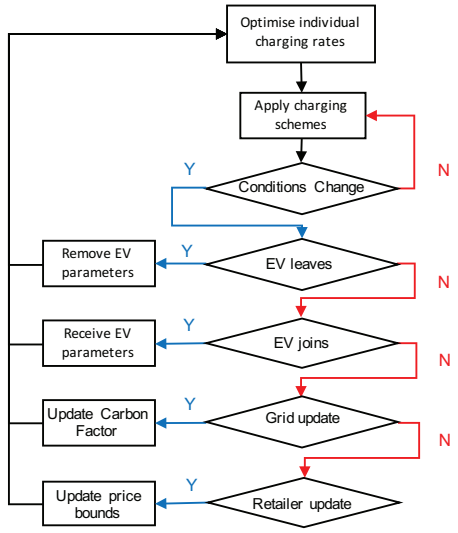

Fig. 3: Schematic overview of the DSM method

4.6 Performance Metrics

To assess the performance of the DSM method, it will be compared to a first-come-first-served (FCFS) allocation whereby, as far as possible, EVs receive their maximum possible charging rate, allocated according to their order of arrival to the road. EVs at the front of the queue receive their maximum charging rate and, when this is no longer possible, the next EV receives the remaining capacity and all those following receive no charge. Furthermore, this method is considered in the case where all of the supply is from the grid, and with renewable integration, separately. The performance of the DSM method will ultimately be assessed by its ability to:

(1) *Control the demand profile*

The UK, and indeed global, demand cycle consists of low demand late at night and early in the morning and much greater demand during the middle of the day - typically containing two distinct peaks. Such a profile is problematic for generation infrastructure since this requires a large installed capacity to accommodate the peaks and an ability to quickly respond to the behaviour of the loads. This leaves much of the capacity unused for large portions of the day and load variability significantly limits the generation techniques that can be used. Flexible loads that can alter their consumption inline with generation, therefore, have the potential to significantly reduce this problem in manufacturing a flatter, more manageable, demand profile. As such, the proposed system should demonstrate the ability to act as a flexible load. That is, reducing consumption when generation is strained and conversely, allowing increased transfer during off-peak times.

(2) *Reduce CO_2 production*

Road transport makes up approximately 20% of EU carbon emissions [39]. This will undoubtedly reduce with increased penetration of EVs. However, in this future scenario, emissions associated with an individual EV's usage will be defined considerably by the generation make-up at time of charging. By introducing flexible loads such as the proposed DRS, significant reductions in associated emissions are expected. In order to realise ambitious carbon emission reduction targets, the ability of DSM methods to contribute to these reductions will undoubtedly make the implementation of such systems appealing for government investment. Performance with respect to CO_2 emissions is, therefore, interrogated.

(3) *Fairly distribute resources*

The expected benefits with respect to (1) and (2) should not come at the expense of system fairness. That is, the disparity in user experience should be kept to a minimum. The following is introduced as a measure of how satisfied a given user is:

$$r_n = \frac{\sum_{t=0}^{T} x_n^{(t)}}{b_n}, \tag{13}$$

where t is the time step and T is the total time that the n^{th} EV is on the DRS. Simply, the total charge received as a proportion of the available battery capacity when entering the road.

To characterise inequalities in user experience, the Gini coefficient is used. Originally used as a measure of income inequality, it can be described as the half of the average absolute difference of all pairs of items in the set scaled by the average or, simply [40],

$$G = \frac{\sum_{i=1}^{N} \sum_{j=1}^{N} |r_i - r_j|}{2N \sum_{i=1}^{N} r_i}. \tag{14}$$

Clearly, if $r_i = r\ \forall\ i \in \boldsymbol{N}$, then $G = 0$, representing complete equality, and if the set only contains a single non-zero value, then G = 1, representing complete inequality.

5 Results and Discussion

This section contains analysis of the performance of the proposed system. The parameters used for simulation are given in Section 5.1, the effects of the DSM method on the demand profile, CO_2 production and fairness are discussed in Sections 5.2, 5.3 and 5.4, respectively.

5.1 Simulation Setup

Historical data was used to simulate the system over a 24-hour period where wind speeds, traffic flow rates and grid make-up exhibit significant variation. Wind speed data was taken from The University of Edinburgh School of Geoscience at one minute intervals throughout the day for a randomly selected day in September 2016 [41]. By incorporating real and fine grained wind speed data, the true intermittency and volatility of the renewable resource can be simulated. The implicit assumption, therefore, is that this day is indicative of typical conditions. In conjunction, a single 1 MW Vergnet wind turbine's wind-power characteristics curve is used to estimate the energy generated from the wind [42]. A linear relationship between wind speed and power output has been assumed between cut-in and cut-out wind speeds.

Traffic flow rates are taken from the M6, recorded by Highways England at 15-minute intervals with the assumption that a third of the traffic flow through the road is over a single lane, in this case the charging lane [43], and a one mile stretch of road is simulated. The composition of the gird's generated electricity was taken from GridWatch at 15-minute intervals [44].

The transformer capacity, $C = 1000$ kW, is chosen arbitrarily such that it constrains the system at several points during the day. By doing so, the performance of the system when the capacity limit is reached can be investigated. Limits on the price of electricity have been set at $£0.10 \leq p \leq £0.30$. This will account for the minimum price necessary for the retailer to cover its costs while capping the upper amount to ensure an unreasonable price is not charged to users. The values chosen are relative to a typical average electricity cost in the UK of $0.12£/kWh$ [45], whilst recognising that due to the value of the service to users, a higher rate can reasonably be expected. A constant velocity of 70 mph has been assumed for each vehicle in line with UK motorway speed limits.

Minimum charging rates for each EV have been chosen randomly with a uniform distribution between 2 kW and 5 kW to recognise that different EV manufacturers will have different lower charging limits. Maximum charging rates vary considerably between EV models. Typical low power cars such as Volkswagen and Nissan models have 50kW maximum charging rates [46] while higher power Telsa models can charge at up to 140 kW in the static case [47]. For the purpose of simulation, charging rates have been modelled as a normal distribution around 75 kW with a standard deviation of 20 kW, capped at 100 kW in line with the findings of the Highways England Feasibility study for dynamic charging [8].

Typical battery sizes for EVs range from 30 kWh to 100 kWh [46]. For simulation, a normal distribution with a mean of 50 kWh and standard deviation 20 kWh has been assigned to the available capacity when entering the road.

A summary of simulation parameters is presented in Table 2. $\mathcal{N}(\mu, \sigma)$ is used to denote a normal distribution with mean, μ, and standard deviation, σ, and $\mathcal{U}(a, b)$ is used to denote a uniform distribution between a and b.

Table 2 Simulation parameters

Parameter	Value
Transformer capacity (kW)	$C = 1000$
Maximum electricity price (£)	$p_{max} = 0.30$
Minimum electricity price (£)	$p_{min} = 0.10$
Car speed (m/s)	$v = 31.3$
Maximum charging rate (kW)	$40 \leq T_n^{(max)} \sim \mathcal{N}(75, 20) \leq 100$
Minimum charging rate (kW)	$2 \leq T_n^{(min)} \sim \mathcal{U}(2, 5) \leq 5$
Available battery capacity (kWh)	$3 \leq b_n \sim \mathcal{N}(50, 20) \leq 100$
Satisfaction parameter	$1 \leq s_n \sim \mathcal{N}(1.5, 0.2) \leq 2$

The profiles of the carbon factor, f, as defined in Section 4, and the traffic flow rate are shown in Figure 4. It can be seen that times of heavy traffic coincide with times of day where the generation is producing high levels of CO_2 - compounding the effect of consuming grid-generated electricity at peak times. This coincidence is due to heavy electricity usage when people wake up and when they return home, which naturally occurs at the times people travel to and from work.

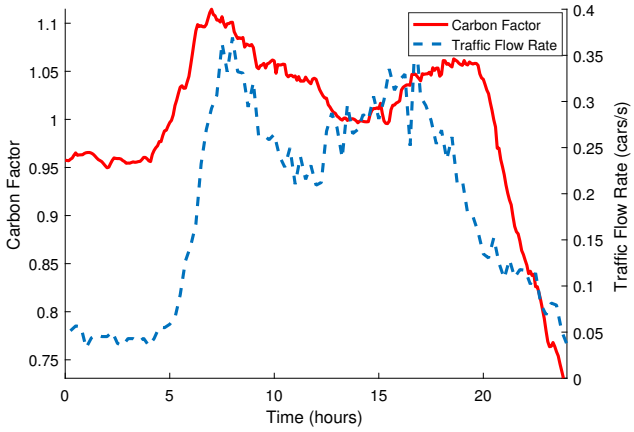

Fig. 4: Carbon factor and traffic flow rate profiles

The DSM method is used with player weights of $\alpha = 0.1$, $\beta = 0.0075$ and $\gamma = 0.8925$ throughout this section except when varying the weights is explicitly stated. These are chosen as a good balance that demonstrates the beneficial operation of the method. The simulation is carried out using *MATLAB*, with the *fmincon* function used to solve the quadratic optimisation problem in (11) at each iteration. In doing so, the Interior-point method is utilised [48]. As the problem in questioned is a convex optimisation problem, as discussed in section 4.4, this convex solver is appropriate. Moreover, by classifying the problem as such, the computational cost is significantly reduced as local optima are, by definition, global optima. When simulating the 24-hour period, the optimisation step takes less that 0.1s throughout the entire simulation using a laptop version of *MATLAB*. As such, it is deemed that the computational cost of the method is small and entirely appropriate for the DRS.

5.2 Demand Profile

The total demand over the 24-hour period is shown in Figure 5 for the proposed DSM method and the FCFS method. The energy supplied to the DRS by local renewable generation is also shown where random variation can be observed. Note that local generation exceeds DRS consumption at various points during off-peak times, and this may be sold back to the grid but is not depicted here. Figure 6 presents the average EV demand and renewable energy supplied in this period for the DSM method.

From Figure 5, it can be seen that, during times of day corresponding to both low traffic flow and low carbon factor, in the periods 0:00-6:00 and 21:00-24:00 as depicted in Figure 4, there is no difference between the FCFS and DSM methods. This is because each EV is receiving its maximum possible transfer rate whilst on the road. The graphs diverge from approximately 6:00 to 20:00. For the FCFS method the transformer capacity is reached at two distinct sections of the day. In the DSM method, lower peaks are observed at these times as a result of taking into account the negative impact of high carbon factor on the overall system utility.

Since the optimisation variable is the energy demanded from the grid, the peak between 7:00-10:00 is distinctly lower than the peak later in the day as renewable generation is also lower. Accordingly, the average EV demand during these times shows noticeable drops, as seen in Figure 6, where it is clear that the average demand follows renewable generation - offset by the optimised grid demand.

It is noted that the volatility of the local generation, and hence the demand profile of the DSM method, is over exaggerated. This is because a direct link between wind speed and turbine power output is used where in reality the output would be somewhat smoother due

to system inertia. For the DSM method, the average price observed throughout the day was found to be $p = 0.1044£/kWh$.

Varying the weights assigned to each player's utility function, α, β and γ from (11), alters the profile observed with the DSM method. Figure 7 displays the resultant daily demand profile at various combinations of α, β and γ. Each scenario is labelled with a number for ease of referencing.

Scenario 2 shows the effect of optimising for the EV users' utilities exclusively. That is, each EV receives its optimum charge rate as per the utility function and the average price is $p = 0.1000£/kWh$ - the minimum constraint. Since no additional benefit is gained for higher transfer rates, each EV receives rate, y_n^*, the rate corresponding to the maximum of the quadratic function, $u_n(y_n, p)$. Scenario 2 shows the effect of introducing the retailer to the system. Here, each EV receives its maximum transfer rate as far as the transformer capacity allows since, for any given EV, once their maximum charge rate is reached then,

$$u_n(p) = y_n^*(b_n - p) - \tfrac{1}{2}sy_n^{*2}, \tag{15}$$

and the corresponding retailer utility is,

$$L_n(y_n, p) = y_n p, \tag{16}$$

so increasing demand at constant price can only increase system utility. Increasing α, therefore, has the effect of pushing the curve up as far as $y_n \neq T_n^{(max)}\ \forall\ n \in \boldsymbol{N}$. Scenario 3 shows the effect of increasing the weight on the regulator's utility where an average price of $p = 0.1045£/kWh$ is observed. Overall demand is decreased, particularly during peak times. This follows from the regulator's utility function. Since, $R \propto f\boldsymbol{X}^2$, it has the greatest effect around the peaks where f is at daily maxima and so indeed is total demand.

In summary, by appropriately weighting the goals of the stakeholders, the profile can be varied considerably. This feature means that the operation of the system can easily be altered for optimum performance in different situations and, practically, these would be set by the regulator.

Substituting (3), (6) and (10) into (11), setting the constants L_{max}, R_{max} and U_{max} to 1, and making use of $x_n = y_n - P_n$, the partial derivatives of the system utility for a single user can be calculated:

$$\frac{\partial F_n}{\partial y_n} = \alpha p + 2\beta(f-1)(P_n - y_n) + \gamma(b_n - p - y_n s), \tag{17}$$

$$\frac{\partial F_n}{\partial p} = y_n(\alpha - \gamma). \tag{18}$$

From this, the effect of the weights on the marginal utility gain with respect to each variable can be seen. From (17), increasing the proportion of renewables supplied, P_n, with constant demand, y_n, increases overall utility given that $f > 1$. Increasing α adds utility at constant price, and, since $y_n \geq P_n$, increasing β always decreases utility. From (18), increasing price at constant demand can only be beneficial if $\alpha > \gamma$ and, therefore, the optimised price for the cases shown is close to the minimum constraint.

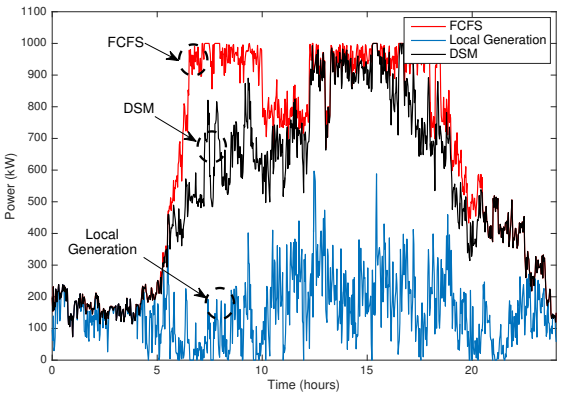

Fig. 5: 24-hour demand profile for FCFS and DSM methods and the energy supplied from local renewable generation

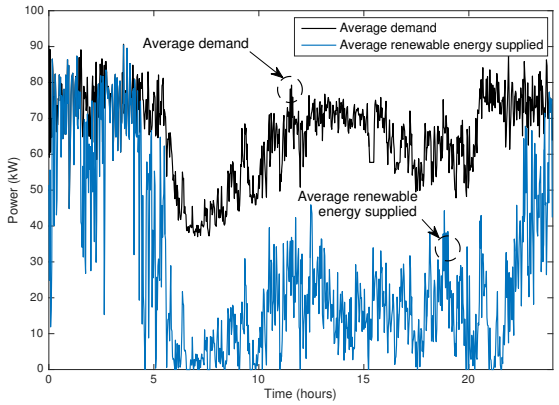

Fig. 6: Average EV demand and renewable energy supplied over 24 hours

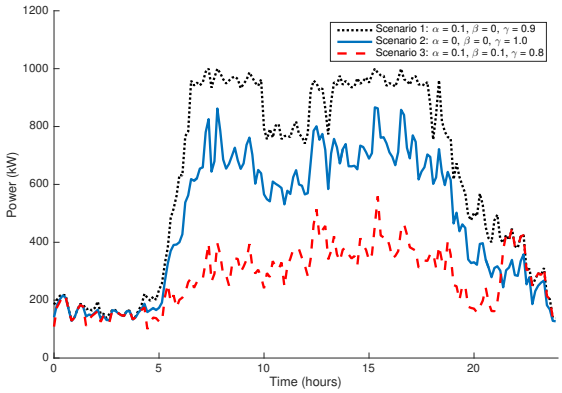

Fig. 7: 24-hour demand for the DSM method with various α, β and γ values

5.3 CO_2 Production

The hourly CO_2 production of the DSM method, alongside FCFS with renewable integration and FCFS grid-only systems are given in Figure 8. During the middle part of the day, when the applications of the two methods diverge, the hourly CO_2 production is materially decreased - particularly around the two peak regions. From 0:00-6:00, and 21:00-24:00, $f < 1$ and therefore the regulator does not act on the system and the FCFS and DSM methods have comparable carbon emissions. In the interval 6:00-21:00, the carbon factor, $f > 1$. As such, the regulator influences the demand during this period. Separation between DSM and FCFS methods is greater around the two peaks where both the carbon factor and system demand are high - in accordance with the regulator's utility function.

The difference between the FCFS system with and without renewables is simply offset by the energy generated locally. From the FCFS, grid-only, curve it can be seen that the CO_2 production follows the demand curve very closely as the load is inflexible.

Over the whole day, the CO_2 production for the three considered cases was 2.54×10^3, 3.25×10^3 and 4.35×10^3 $kgCO_2$ equivalent, respectively. There is a 21.8% reduction in CO_2 production over the whole day as a result of applying the proposed DSM method over a FCFS system and a 41.6% decrease when compared to a FCFS, grid-only system.

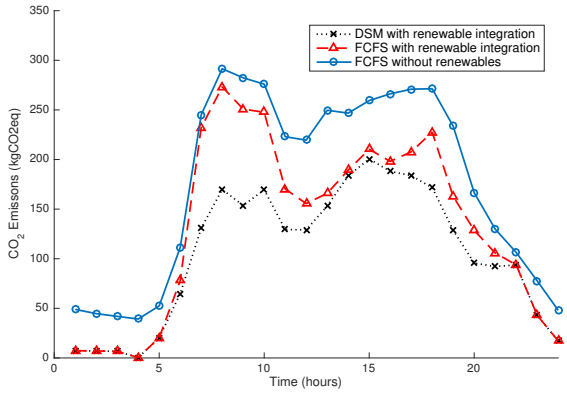

Fig. 8: Hourly CO_2 production profiles for three considered cases

Figure 9 displays CO_2 emissions with the DSM method where the theoretical power output of the wind turbine has been increased from its normal level to double that in 10 increments, at every time step. As such, this provides some insight into the effect of adding more local generation capacity in the same wind conditions.

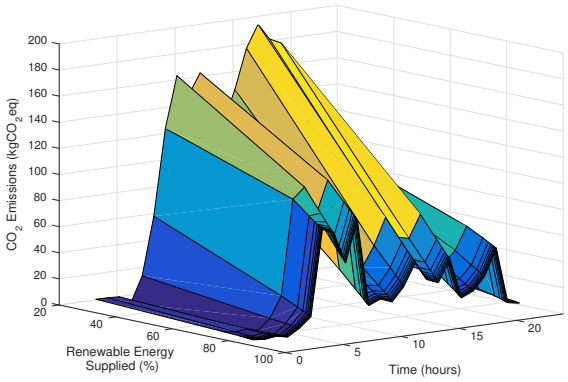

Fig. 9: Hourly CO_2 production profile with incremental 10% increases in the power supplied by local renewable energy generation

Notably, for small increases in the amount of renewable energy supplied, significant reduction in emissions occur and, conversely, as renewables approach 100%, the marginal gains diminish. That is, each additional increase in the local energy generated has decreasing effect in reducing emissions. This can be seen here as the lines representing each incremental increase become closer together.

In addition, the difference in emissions between successive increments is larger around the peaks. This follows as greater gains can be expected when the average renewable power and consumption become closer together. At the off-peak times, the average renewables available quickly becomes greater than average consumption but, due to variability in the local generation, grid electricity is still required to supplement demand. This follows as increasing installed capacity does not reduce the volatility of the supplied power.

The benefits, then, are clear with respect to carbon emissions as it is shown that the DSM method can significantly reduce emissions and, furthermore, small amounts of local generation can produce significant benefits. This makes the system particularly attractive to authorities responsible for UK road infrastructure with ambitious CO_2 reduction targets.

5.4 Fairness

The relative satisfaction of each EV, r, as defined in Equation 13, is the ratio of the amount of charge received whilst on the road to the available battery capacity when entering the road. The distribution

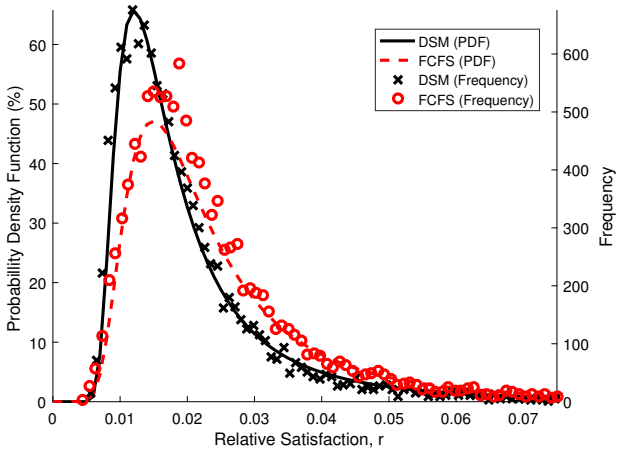

Fig. 10: Distribution of user relative satisfaction

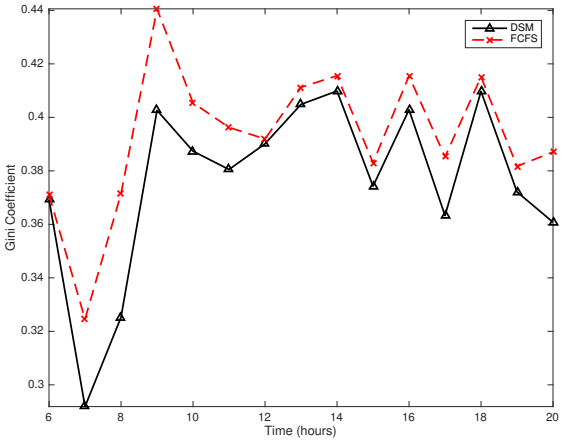

Fig. 11: Gini coefficient for DSM and FCFS methods

of relative satisfaction for the DSM and FCFS methods are shown in Figure 10 for the period 6:00-20:00. Outside of this interval the fairness achieved is the same for both methods as each EV receives its maximum charging rate when few EVs are on the road. The achieved values of relative satisfaction were distributed into 500 equal bins and the frequency of values in each bin is plotted. In addition, the data was fitted to a 'Generalised Extreme Value' distribution which is plotted on top of the raw values. For clear viewing, values corresponding to $r > 0.075$ have not been included in the figure as these are near zero. The hourly average Gini coefficient, as defined in (14), for the relative satisfaction metric is plotted for the DSM and FCFS allocation methods in Figure 11 for the same period.

From Figure 10, it can be seen that the expected value of r is marginally lower for the DSM method as expected since the overall demand of the system is materially reduced with $r_{DSM} = 0.0251 \pm 0.0338$ as opposed to $r_{FCFS} = 0.0295 \pm 0.0397$, within a single standard deviation. The spread of values for the random allocation method is greater than that of the DSM method. This means that more EVs are receiving a proportionally large or small amount of charge and the disparity between user experience is greater. For this reason, it can be seen that the probability distribution follows the FCFS data points less closely since the distribution is skewed by non-zero frequencies at high values of r.

From Figure 11 it can be seen that, during peak hours, when DSM significantly reduces the overall power transfer, system fairness is not adversely effected. In fact, it is improved with an average reduction of 4.32% in the Gini coefficient in this period.

In summary, the changes made to the daily demand profile and CO_2 emissions caused by the DSM method do not negatively impact user experience to a considerable extent.

6 Conclusion

The proposed DSM method produces a number of benefits for the future DRS. By modelling a regulator in the multi-objective optimisation problem, the system acts to reduce the power drawn from the grid when carbon emissions per unit energy are high. Since this typically occurs during peak times, demand reduces during these intervals which produces a smoother, more manageable daily profile. In this way, the DRS acts as a variable load to the power grid. When compared to a FCFS allocation method, with integrated renewables and without, the DSM method reduced CO_2 emissions by 22% and 42% respectively. Furthermore, the described benefits do not significantly impact the relative satisfaction of the users and system fairness is shown to improve by 4.32%.

7 Limitations and Future Work

While the described system has a number of benefits, it is recognised that there are limitations to the proposed scheme. Specifically, in modelling a DSM method for application in dynamic charging, focus is on demonstrating how such a system can operate under varying conditions. In doing so, the approach to balancing the objectives of the regulator, retailer and EV users has not been explored. In addition, a simplistic approach has been taken with regards to setting the electricity price which results in near constant price during the simulated period. Therefore, it is suggested this work be extended to incorporate a robust time-of-use pricing scheme and a framework for setting weights assigned to players' goals such that all parties are satisfied. Finally, it is advised that the capabilities of hardware necessary to realise such a system be interrogated. That is, the controllers required to provide each EV with a unique charging rate and the low latency vehicle sensor and communication infrastructure necessary to realise the proposed system.

8 Acknowledgments

This work was supported by the UK EPSRC under Grant EP/P005950/1, and in part by the European Union's Horizon 2020 Research and Innovation Staff Exchange Programme under the Marie Sklodowska-Curie grant agreement No. 734325 TESTBED project.

9 References

1 Society of Motor Manufacturers and Traders, "EV and AFV Registrations," January 2018. [Online]. Available: https://www.smmt.co.uk/2018/02/january-ev-registrations/ (Accessed: 10/03/18)

2 European Environment Agency, "Electric Vehicles in Europe," Report, Copenhagen, Denmark, 2016. [Online]. Available: https://www.eea.europa.eu/publications/electric-vehicles-in-europe (Accessed: 10/03/18)

3 National Grid, "Future Energy Scenarios," Report, Warwick, UK, July 2017. [Online]. Available: http://fes.nationalgrid.com/media/1253/final-fes-2017-updated-interactive-pdf-44-amended.pdf (Accessed 08/03/18)

4 European Parliment: Directorate-General For Internal Policies, "Reseach for TRAN Commitee - Self-piloted cars the future of transport?" Study, European Parliment, Brussels, 2016. [Online]. Available: http://www.europarl.europa.eu/RegData/ (Accessed: 10/03/18)

5 UK Department for Transport, "Research on the Impacts of Connected and Autonomous Vehicles on Traffic Flow," Summary Report, St Leonards on Sea, UK, May 2016. [Online]. Available: https://www.gov.uk/government/uploads/system/uploads (Accessed: 10/03/18)

6 E. Bulut and M. C. Kisacikoglu, "Mitigating Range Anxiety via Vehicle-to-Vehicle Social Charging System," in *Proc. IEEE 85th Vehicular Technology Conference (VTC Spring)*, Sydney, NSW, Australia, June 2017, pp. 1–5.

7 The International Council on Clean Energy Transportation, "Electric Vehicles: Literature Review of Technology Costs and Carbon Emissions," Literature Review, San Francisco, CA, USA, July 2016. [Online]. Available: www.theicct.org/sites/default/files/publications (Accessed 10/03/18)

8 Transport Research Laboratory, "Highways England Feasibility Study: Powering Electric Vehicles on England's Major Roads," Feasibility Report, July 2015. [Online]. Available: http://assets.highways.gov.uk/ (Accessed: 10/03/18)

9 J. Gill, P. Bhavsarb, M. Chowdhuryb, J. Johnsonc, J. Taibera, and R. Friesd, "Infrastructure Cost Issues Related to Inductively Coupled Power Transfer for Electric Vehicles," in *Proc. 5th International Conference on Sustainable Automotive Technologies*, vol. 32, Hasselt, Belgium 2014, pp. 545–552.

10 B. J. Limb, T. H. Bradley, B. Crabb, R. Zane, C. McGinty, and J. C. Quinn, "Economic and Environmental Feasibility, Architecture Optimization, and Grid Impact of Dynamic Charging of Electric Vehicles Using Wireless Power Transfer," in *Proc. 6th Hybrid and Electric Vehicles Conference (HEVC)*. London, UK: IET, November 2016, pp. 1–6.

11 S. Jeong, Y. J. Jang, and D. Kum, "Economic Analysis of the Dynamic Charging Electric Vehicle," *IEEE Transactions on Power Electronics*, vol. 30, no. 11, pp. 6368 – 6377, April 2015.

12 X. Mou, O. Groling, A. Gallant, and H. Sun, "Energy Efficient and Adaptive Design for Wireless Power Transfer in Electric Vehicles," in *Proc. IEEE 83rd Vehicular Technology Conference (VTC Spring)*, Nanjing, China, May 2016.

13 S. Kuutti, S. Fallah, K. Katsaros, M. Dianati, F. Mccullough, and A. Mouzakitis, "A Survey of the State-of-the-Art Localisation Techniques and Their Potentials for Autonomous Vehicle Applications," *IEEE Internet of Things Journal*, vol. PP, March 2018.

14 A. Gil, P. Sauras-Perez, and J. Taiber, "Communication Requirements for Dynamic Wireless Power Transfer for Battery Electric Vehicles," in *Proc. IEEE International Electric Vehicle Conference (IEVC)*, Florence, Italy, December 2014.

15 A. Echols, S. Mukherjee, M. Mickelsen, and Z. Pantic, "Communication Infrastructure for Dynamic Wireless Charging of Electric Vehicles," in *Proc. IEEE Wireless Communications and Networking Conference (WCNC)*, San Francisco, CA, USA, March 2017, pp. 1–6.

16 M. Pazos-Revilla, M. Pazos-Revilla, S. Gunukula, T. N. Guo, M. Mahmoud, and X. Shen, "Privacy-Preserving Physcial-Layer-Assisted Charging Authorization Scheme for EV Dynamic Charging Systems," *IEEE Transactions on Vehicular Technology*, vol. PP, December.

17 T. V. Theodoropoulos, I. G. Damousis, and A. J. Amditis, "Demand-Side Management ICT for Dynamic Wireless EV Charging," *IEEE Transactions on Industrial Electronics*, vol. 63, no. 10, pp. 6623 – 6630, October 2016.

18 H. Li, G. Dán, and K. Nahrstedt, "FADEC: Fast Authentication For Dynamic Electric Vehicle Charging," in *Proc. 2013 IEEE Conference on Communications and Network Security (CNS)*, no. 370, National Harbor, MD, USA, 2013, p. 369.

19 International Organization for Standardization, "ISO/IEC 15118: Vehicle to grid communication interface." [Online]. Available: http://www.iso.org/iso/catalogue_detail.htm?csnumber=55366 (Accessed: 05/08/2018)

20 Y. Zheng and L. Jian, "Smart Charging Algorithm of Electric Vehicles Considering Dynamic Charging Priority," in *Proc. IEEE International Conference on Information and Automation (ICIA)*, Ningbo, China, August 2016, pp. 555–560.

21 T. Theodoropoulos, Y. Damousis, and A. Amditis, "A Load Balancing Control Algorithm for EV Static and Dynamic Wireless Charging," in *Proc. IEEE 81st Vehicular Technology Conference (VTC Spring)*, Glasgow, UK, May 2015, pp. 1–5.

22 A.-H. Mohsenian-Rad, V. W. S. Wong, J. Jatskevich, R. Schober, and A. Leon-Garcia, "Autonomous Demand-Side Management Based on Game-Theoretic Energy Consumption Scheduling for the Future Smart Grid," *IEEE Transactions on Smart Grid*, vol. 1, no. 3, pp. 320–331, November 2010.

23 L. Zhang and Y. Li, "A Game-Theoretic Approach to Optimal Scheduling of Parking-Lot Electric Vehicle Charging," *IEEE Transactions on Vehicular Technology*, vol. 65, no. 6, pp. 4068–4078, June 2016.

24 Z. Zhu, S. Lambotharan, W. H. Chin, and Z. Fan, "A Mean Field Game Theoretic Approach to Electric Vehicles Charging," *IEEE Access*, vol. 4, pp. 3501–3510, June 2016.

25 A. Ovalle, A. Hably, and S. Bacha, "Optimal Management and Integration of Electric Vehicles to the Grid: Dynamic Programming and Game Theory Approach," in *Proc. IEEE International Conference on Industrial Technology (ICIT)*, Seville, Spain, March 2015, pp. 2673–2679.

26 W. Tushar, W. Saad, V. Poor, and D. Smith, "Economics of Electric Vehicle Charging: A Game Theoretic Approach," *IEEE Transactions on Smart Grid*, vol. 3, no. 4, pp. 1767–1778, December 2012.

27 S.-G. Yoon, Y.-J. Choi, J.-K. Park, and S. Bahk, "Stackelberg-Game based Demand Response for At-Home Electric Vehicle Charging," *IEEE Transactions on Vehicular Technology*, vol. 65, no. 6, pp. 4172–4184, June 2016.

28 Z. Yang, K. Li, and A. Foley, "Computational scheduling methods for integrating plug-in electric vehicles with power systems: A review," *Renewable and Sustainable Energy Reviews*, vol. 51, pp. 396 – 416, 2015.

29 M. Babar, T. Taj, I. Ahamed, and A.-A. E.A, "The Conception of the Aggregator in Demand Side Management for Domestic Consumers," *International Journal of Smart Grid and Clean Energy*, vol. 2, no. 3, pp. 371–375, January 2013.

30 J. Hu, H. Morais, T. Sousa, and M. Lind, "Electric vehicle fleet management in smart grids: A review of services, optimization and control aspects," *Renewable and Sustainable Energy Reviews*, vol. 56, pp. 1207 – 1226, 2016.

31 E. T. Lau, Q. Yang, G. A. Taylor, A. B. Forbes, P. Wright, and V. N. Livina, "Optimization of Carbon Emissions in Smart Grids," in *Proc. 49th International Universities Power Engineering Conference (UPEC)*, Cluj-Napoca, Romania, September 2014, pp. 1–4.

32 T. Theodoropoulos, A. Amditis, J. Sallán, H. Bludszuweit, B. Berseneff, P. Guglielmi, and F. Deflorio, "Impact of Dynamic EV Wireless Charging on the Grid," in *Proc. IEEE International Electric Vehicle Conference (IEVC)*, Florence, Italy, December 2014, pp. 1–7.

33 K. Deb, A. Pratap, S. Agarwal, and T. Meyarivan, "A Fast and Elitist Multiobjective Genetic Algorithm: NSGA-II," *IEEE Transactions on Evolutionary Computation*, vol. 6, no. 2, pp. 182–197, April 2002.

34 Z. Moghaddam, I. Ahmad, D. Habibi, and Q. V. Phung, "Smart Charging Strategy for Electric Vehicle Charging Stations," *IEEE Transactions on Transportation Electrification*, vol. 4, no. 1, pp. 76 – 88, March 2018. [Online]. Available: https://ieeexplore.ieee.org/document/8039201/

35 H. Turker, V. Pirsan, S. Bacha, D. Frey, J. Richer, and P. Lebrusq, "Heuristic Strategy for Smart Charging of Plug-In Electric Vehicle in Residential Areas: Variable Charge Power," in *Proc. 2014 International Conference on Renewable Energy*

Research and Application (ICRERA), Milwaukee, WI, October 2014, pp. 938–944.
36 J. Rezgui and S. Cherkaoui, "Smart charge scheduling for evs based on two-way communication," in *Proc. 2017 IEEE International Conference on Communications (ICC)*, Paris, May 2017, pp. 1–6.
37 D. Li, W.-Y. Chiu, H. Sun, and H. V. Poor, "Multiobjective optimization for demand side management program in smart grid," *IEEE Transactions on Industrial Informatics*, vol. 14, no. 4, pp. 1482–1490, 2018.
38 Parlimentary Office of Science and Technology, "Carbon Footprint of Electricity Generation," October 2006. [Online]. Available: https://www.parliament.uk/documents/post/postpn_383-carbon-footprint-electricity-generation.pdf (Accessed: 10/03/18)
39 E. Comission, "Road transport: Reducing CO2 emissions from vehicles." [Online]. Available: https://ec.europa.eu/clima/policies/transport/vehicles_en#tab-0-0 (Accessed: 11/03/18)
40 R. Carvalho, L. Buzna, R. Gibbens, and F. Kelly, "Critical Behaviour in Charging of Electric Vehicles," *New Journal of Physics*, vol. 17, September 2015.
41 The University of Edinburgh, "Weather station data," August 2016. [Online]. Available: https://www.ed.ac.uk/geosciences/weather-station/weather-station-data (Accessed 10/03/18)
42 Wind Turbine Models, "Vergnet GEV HP 1 MW." [Online]. Available: https://www.en.wind-turbine-models.com/turbines/435-vergnet-gev-hp-1mw (Accessed 10/03/18)
43 H. England, "Traffic flow data," August 2017. [Online]. Available: http://tris.highwaysengland.co.uk/detail/trafficflowdata (Accessed 10/03/18)
44 The National Grid, "G.B. National Grid Status," August 2017. [Online]. Available: http://www.gridwatch.templar.co.uk/download.php (Accessed 10/03/18)
45 UK Power, "Gas & Electricity Tariff Prices per kWh." [Online]. Available: https://www.ukpower.co.uk/home_energy/tariffs-per-unit-kwh (Accessed 10/03/18)
46 E. V. Database. [Online]. Available: https://ev-database.uk/ (Accessed: 13/13/18)
47 Plugless, "Tesla charging." [Online]. Available: https://www.pluglesspower.com/learn/tesla-model-s-charging-home-public-autonomously/ (Accessed: 10/03/18)
48 MathWorks, "Constrained Nonlinear Optimization Algorithms." [Online]. Available: https://uk.mathworks.com/help/optim/ug/constrained-nonlinear-optimization-algorithms.html#brh9swj (Accessed: 05/08/2018)